2007-01-01

Vibrational Characterisation and Fluorescence Optimisation of Polycyclic Polymers

Luke O'Neill
Dublin Institute of Technology

Patrick Lynch
Dublin Institute of Technology

Mary McNamara
Dublin Institute of Technology, Mary.McNamara@dit.ie

Hugh J. Byrne
Dublin Institute of Technology, Hugh.byrne@dit.ie

Recommended Citation

O'Neill, L., Lynch, P., McNamara, M., Byrne, H.: Vibrational Characterisation and Fluorescence Optimisation of Polycyclic Polymers. J. Phys. Chem. B, 2007, 111 (28), pp 7999–8005 DOI: 10.1021/jp071393s

Vibrational Characterization and Fluorescence Optimization of Polycyclic Polymers

Luke O'Neill,*,† Patrick Lynch,‡ Mary McNamara,‡ and Hugh J. Byrne†

FOCAS Institute, School of Physics and School of Chemical and Pharmaceutical Sciences, Dublin Institute of Technology, Kevin Street, Dublin 8, Ireland

Received: February 19, 2007; In Final Form: May 9, 2007

A systematic series of polycyclic novel polymers was studied by Raman spectroscopy. The effect of the sequential introduction of polycyclic aromatic ring substituents into the delocalized backbone was examined in relation to the variation of the relative ring breathing and stretching as well as the vinyl stretch frequencies. Replacement of the phenyl units by higher order acene moieties such as naphthyl and anthryl results in a shift of the characteristic stretching frequencies, and analysis of the vinyl stretch leads to the confirmation that higher order acene substitution into the delocalized backbone substantially weakens the vinyl bond. Semiquantitative integrated Raman analysis shows a well-defined variation of the vibrational characteristics with structure. The structural variation of the integrated Raman intensity elucidates the effect of the electronic and vibrational decoupling introduced by the continual systematic acene substitution and points toward the ability to tailor the vibrational characteristic of the polymeric systems much the same as the electronic characteristics are manipulated. Relative fluorescence yields calculated for absorption and fluorescence spectroscopy can be seen to be well-correlated with integrated Raman intensities, implying that the reduction of the vibrational intensity limits the avenues of nonradiation, hence optimizing the fluorescence yield.

Introduction

For the past 40 years, inorganic materials such as silicon, gallium arsenide, and metals such as copper and aluminum have dominated the electronics industry. However, a trend has been growing to improve the semi-conducting, conducting, and light emissive properties of organics though novel synthesis and self-assembly techniques.[1−10] For the growth in the electronics industry to be maintained, it is clear that innovative organic materials have an increasingly important role to play. The ability to optimize the properties of organic materials through chemical modification has already provided much needed solutions to many problems, but this is just the beginning.[11]

Far outweighing the practical advantages, the ability to vary and tune optical and electronic properties enables structure−property relationships to be derived to aid material optimization, as well as the realization of a fundamental understanding of the underlying physical processes in these materials. To this end, systematic studies have provided a platform for the optimization of both the electronic properties and an extension into vibrational characteristics. Oligomer series can be used to demonstrate the systematic variation of electronic properties with chemical structure.[12−14] Furthermore, similar structure−property relationships have been demonstrated in the electronic−vibrational coupling in these systems, evident in the form of Stokes shifts and further manifested in the Raman activity.[15] Such a systematic study has been extended to the polymer series shown in Figure 1. Clear structure−property relationships can be illustrated for both optical absorption and fluorescence and can be modeled by use of a simple system based on the relative contributions of the aryl units to the backbone conjugation across the vinyl bond.[16]

By analogy to the model of Meier et al.,[17,18] used to explain the electronic properties of donor−$[\pi]_n$−acceptor oligomers, the polymer series can be considered in terms of oligomers with an acene group of varying length with endgroups that can be [vinyl-phenyl] (**1**, **2**, and **4**) or [vinyl-naphthyl] (**2**, **3**, and **5**). The electronic properties are determined by a combination of the increasing conjugation of the central acene unit and the electronic contribution across the vinyl bond. Although the larger acene units are in themselves more conjugated, their inclusion results in a decreased coupling across the vinyl bond. Thus, the alternating blue-shift to red-shift on going from **1** to **2** to **4** can be understood.[16]

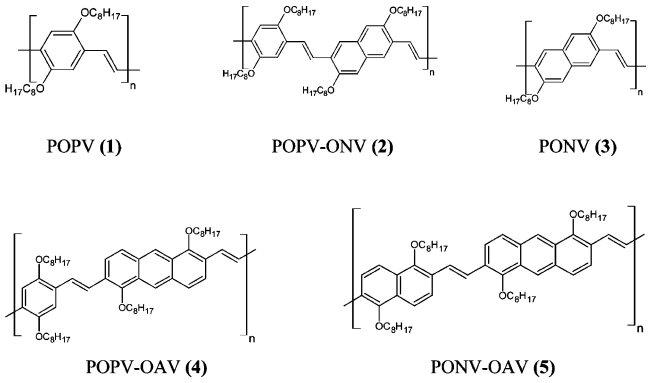

Figure 1. Polymer structures **1**−**5**.

The polymer systems alternatively can be considered in terms of the electron transfer across the vinyl linkage. In this case, the conjugated linker is of constant length, and the nature of the (substituent) terminal groups is varied. This allows the relative conjugation across the whole system to be gauged in terms of the electron donating contributions of the endgroups, and as such, as these groups are varied, the conjugation will be increased or decreased. The electron affinity is chosen as the parameter that can be used to represent changes in the backbone.[16] The energetics of the total system, EA_{total}, can be separated into two distinct parts: (i) the electron donating/accepting contribution of both the substituent units (i.e., phenyl,

* Corresponding author. Tel.: +353-1-4022817; fax: +353-1-4024999; e-mail: Luke.oneill@dit.ie.
† School of Physics.
‡ School of Chemical and Pharmaceutical Sciences.

10.1021/jp071393s CCC: $37.00
Published on Web 06/20/2007

naphthyl, and anthryl) to the linking vinyl bond, EA_{vinyl}, and (ii) the contribution of both substituent groups individually, EA_{subst}. Thus

$$EA_{vinyl} = (EA_{\pi} + EA_{B}) + (EA_{\pi} + EA_{A}) \quad (1)$$

$$EA_{subst} = (EA_{B} + EA_{A})\omega \quad (2)$$

$$EA_{total} = EA_{vinyl} - EA_{subst} \quad (3)$$

where EA_{π} is the electron affinity of the linker vinyl unit and EA_A and EA_B are the electron affinities of the substituent endgroups. ω is a constant that compensates for the fact that the interaction of the nearest neighbor substituent is considered rather than the extended chain.

It has been demonstrated that the optical band gap as measured by UV−vis absorption and photoluminescence of the systems is well-correlated with the parameter EA_{total}.[16] Furthermore, the Stokes shift has been demonstrated to be well-correlated with the contribution across the vinyl bond, EA_{vinyl}, indicating that the electronic−vibrational coupling in these systems is well-definable.

The aim of this study is to extend the vibrational study performed for the phenyl and acene oligomer series[15] to this family of systematically structurally varied polymers. The insertion of the naphthyl and anthryl groups affects the electronic distribution, but it is further anticipated that the differing vibrational frequencies should decouple the oscillators along the backbone, reducing the vibrational coherence and thus the electronic−vibrational coupling. Raman spectroscopy is the primary experimental technique employed, and vibrational intensities will be correlated with Stokes shift to see if the Stokes shift can be used as an indication of vibrational activity as shown for short chain systems. Thus, this will allow examination of the variation of the electronic−vibrational coupling shown by the polymers and whether it has a direct bearing on the fluorescence yield by restricting nonradiative decay, essentially providing vibrational confinement.

Experimental Procedures

The polymer systems (Figure 1) investigated were poly(2,5-dioctyloxy)-1,4-phenylvinylene), POPV (**1**); poly(2,5-dioctyloxy)1,4-phenylenevinylene-*co*-(1,5-dioctyloxy)-2,6-naphthylenevinylene), POPV-ONV (**2**); poly(1,5-dioctyloxy)-2,6-naphthylenevinylene), PONV (**3**); poly(2,5-dioctyloxy-1,4-phenylenevinylene)-*co*-(1,5-dioctyloxy-2,6-anthracenevinylene), POPV-OAV (**4**); and poly(2,5-dioctyloxy-1,5-naphthylenevinylene)-*co*-(1,5-dioctyloxy-2,6-anthracenevinylene), PONV-OAV (**5**). Synthesis of the polymers **1**−**5** has been described elsewhere.[19,20] The polymers were prepared in a chloroform solution of molarity $\approx 10^{-6}$ for solution Raman measurements.

Raman spectroscopy was performed using an Instruments SA (Jobin-Yvon) Labram 1B confocal Raman imaging microscope system. A helium-neon (632.8 nm/11 mW) light source was used. The light was imaged to a diffraction-limited spot via the objective lens of an Olympus BX40 microscope. All experiments were carried out at room temperature (300 K). For Raman spectroscopy, the polymer solutions were examined in thin NMR tubes. A ×10 objective lens was used to maximize the focal depth and so sample the bulk of the solution.

Concentration dependent studies were undertaken to ensure that the samples were unaffected by aggregation.[19] Absorption spectroscopy was carried out using a PerkinElmer Lambda 900 UV−vis NIR absorption spectrometer. The luminescence measurements were performed using a PerkinElmer LS55 luminescence spectrometer. These measurements were used to calculate relative fluorescence yields.

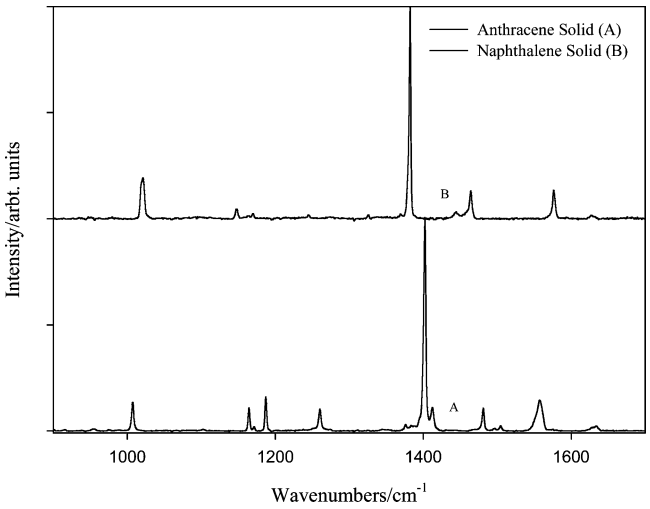

Figure 2. Raman spectra of anthracene and naphthalene (offset for clarity).

Results and Discussion

As can be seen from Figure 1, the polymers studied consist of a series of polycyclic polymers in which a larger acene unit is systematically inserted into the backbone. To fully understand the Raman characteristics of the polymers, it is important to first analyze the Raman signatures of the isolated moieties. For this purpose, the Raman spectra of both naphthalene and anthracene are illustrated in Figure 2.

The naphthalene and anthracene moieties are characterized by a weak C−H stretching band near 3000 cm^{-1} and by bands near 900−1000 and 1500−1600 cm^{-1}, which are ring breathing and stretching, respectively.[22] The other ring associated band occurs at 1200 cm^{-1} for para substituted benzene derivatives. The one other significant band is at 1300 cm^{-1}, which corresponds to the C═C bond stretch that links the phenyl units, and this shows a similar length dependence. A characteristic Raman vibrational frequency that is unique to naphthalene can be found at ∼1380 cm^{-1} and similarly for anthracene at ∼1400 cm^{-1}. These characteristic vibrations will help in the assignment of vibrational modes in the polymer spectra.

The Raman spectra of polymers **1**−**5** are shown in Figure 3, offset for clarity. The main PPV features, present in all, are the ring vibration, ring stretch, and vinyl stretch at ∼1200, 1580, and 1620 cm^{-1}, respectively. The POPV (**1**) Raman spectrum will provide the basis on which all other polymers will be compared, and as such, the relative effects of the continual substitution of more conjugated acene subunits can be gauged accurately. To this end, the additional features and spectral shifts introduced by the incorporation of the higher order acene units can be accessed with reference to a POPV spectrum with two octyloxy side chains.

The Raman spectrum of POPV-ONV (**2**) exhibits all the main peaks ascribed to POPV. However, the inclusion of the alternating phenyl/naphthyl unit into the POPV (**1**) backbone results in the addition of a new spectral feature at ∼1400 cm^{-1}, which can be attributed to the naphthyl ring stretch (Figure 2). The inclusion of the more conjugated naphthyl units also has a significant effect on the peak positions of the ring related stretch and vibrations. Both ring vibration and stretch are shown to move to higher energies, suggesting that the naphthyl inclusion

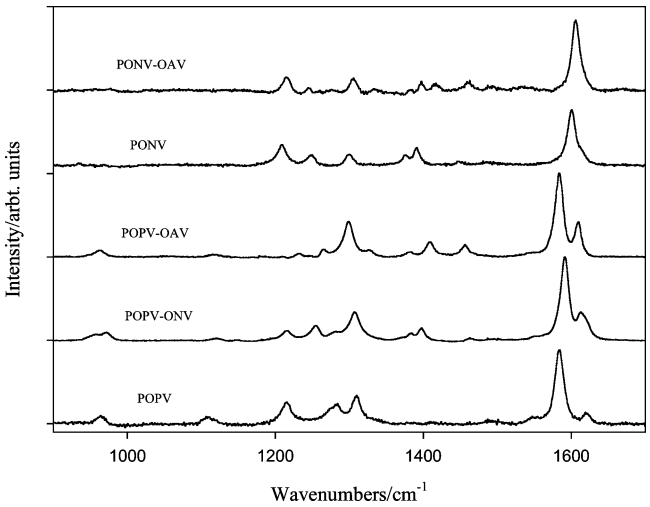

Figure 3. Raman spectra of polymers studied (offset for clarity).

has the effect of increasing the conjugation of the ring structure present in the backbone. This is, of course, expected as it can be seen in the shift of the Raman modes with increased acene length. However, the most interesting spectral change to arise from the change from POPV (**1**) to POPV-ONV (**2**) is the shift of the vinyl stretch. In POPV, the features in the region 1560−1630 cm^{-1} are best fitted by Voigt functions at 1584 and 1619 cm^{-1}, respectively, which can be attributed to the ring and vinyl stretch, respectively. This is consistent with ring and vinyl frequencies reported in PPV derivatives.[23,24]

A close examination of POPV-ONV reveals that features in the region of 1560−1630 cm^{-1} are best fitted by two Voigt functions at 1591 and 1616 cm^{-1}, the latter of which is assigned to the vinyl stretch. The next polymer in the series was PONV, which contained a partially masked vinyl stretch. Because of the proximity of the vinyl and ring stretch, the relevant peak positions were obtained through a thorough Voigt analysis. The fits were preformed using Peakfit. The introduction of a further naphthyl making the polymer a complete naphthalene vinylene copolymer, PONV (**3**), resulted in a further downshift for the vinylene stretch (1612.9 cm^{-1}) as shown in Figure 4. The softening of the vinyl mode in comparison to that of POPV is consistent with the interpretation of the variation of the electronic properties as being a result of a partial disruption of the conjugation across the vinyl bond, although the naphthalene unit is in itself more conjugated.[16]

Having exhausted the possible combination of naphthalene polymers, the next step was to examine the effect of substituted higher order acenes (anthracene) into the backbone to see if the trends were maintained. The inclusion of an alternating anthryl/phenyl unit into the backbone in POPV-OAV (**4**) resulted in the feature at ∼1410 cm^{-1}, which can be attributed to the anthryl ring stretch.[22] The inclusion of the more conjugated anthryl units also has a significant effect on the peak positions of the ring related stretches and vibrations. The ring stretch that was last seen at 1600 cm^{-1} for PONV has shifted to a lower energy of 1592 cm^{-1}, just 8 cm^{-1} higher that the original POPV. The vinyl stretch is evident at 1614 cm^{-1}. This value for the vinyl stretch is reduced from the original POPV but larger in energy than that of the doubly substituted naphthyl polymer.

The Raman spectrum of PONV-OAV (**5**) shows both anthryl and naphthyl related bands due to the inclusion of an alternating anthryl/naphthyl unit into the backbone and results spectral features at ∼1410−1460 cm^{-1}, which can be attributed to a

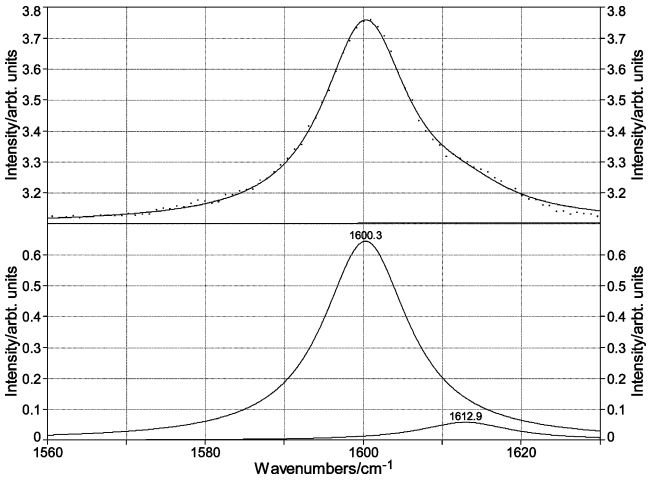

Figure 4. Voigt fit of PONV; dotted line shows original spectrum, and black line shows fit (upper) and independent Voigt (lower).

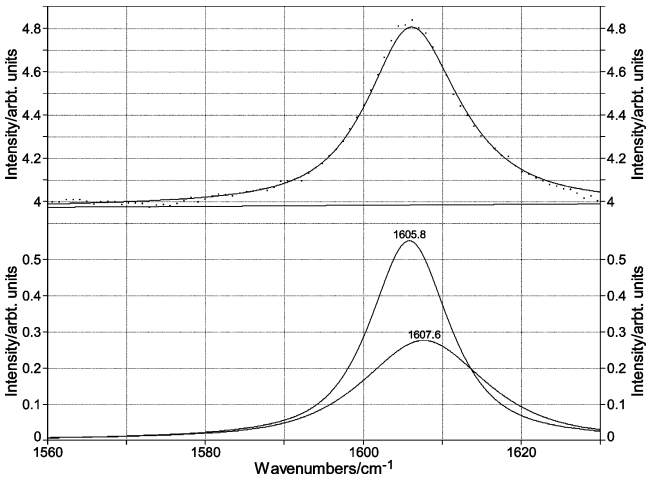

Figure 5. Voigt fit of PONV-OAV; dotted line shows original spectrum, and black line shows fit (upper) and independent Voigt functions (lower).

combination of naphthyl and anthryl ring stretches. The inclusion of both naphthyl and anthryl units has a significant effect on the peak positions of the ring related stretch and vibrations. The ring stretch has shifted to a higher energy found at 1605 cm^{-1}. The vinyl feature appears absent, which suggests that the vinyl vibration has been reduced in energy to be masked now by the ring stretch. Figure 5 illustrates that the features in the region of 1560−1630 cm^{-1} is best fitted by two Voigt functions at 1605.8 and 1607.6 cm^{-1}. The feature at 1607.6 cm^{-1} is assigned to the partially masked vinyl stretch. Again, it can be seen that as with the electronic features, the vinyl stretch seems to mirror the disruption in conjugation and hence the band gap.

The Voigt fits to the Raman spectra indicate that the vinyl bond does indeed soften with the continued introduction of the larger acene units into the polymer backbone. The polymers in which the vinyl stretch clearly can be seen (i.e., POPV, POPV-ONV, and POPV-OAV) also show that a single Voigt function accurately fits the ring stretching peak. In the spectra of the other two polymers, PONV and PONV-OAV, where the vinyl stretch was thought to be absent or masked, to accurately account for their peak shape, two separate Voigt functions were needed. This shows that the vinyl peak has indeed been incorporated into the ring stretch peak but clearly can be seen with the curve fitting analysis. All vinyl and ring stretching frequencies can be found in Table 1. With the analysis of the peak position yielding an interesting variation in the bond

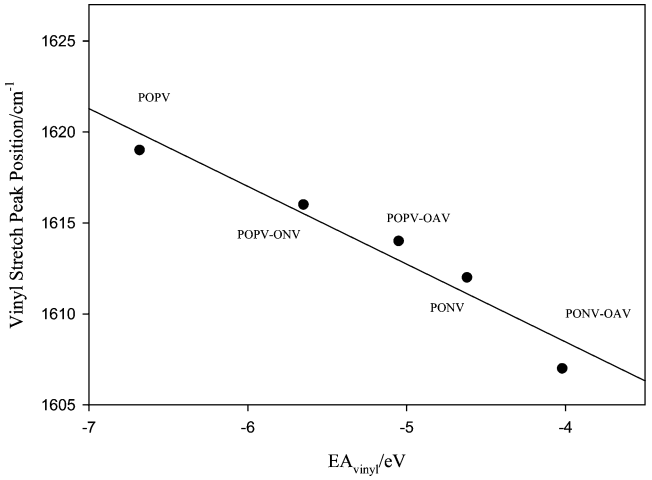

Figure 6. Position of the vinyl stretch plotted against EA_{vinyl}. The solid line is a guide for the eye.

TABLE 1: Vinyl and Ring Stretch Frequencies

polymer	ring stretch (cm^{-1})	vinyl stretch (cm^{-1})
POPV	1584	1619
POPV-ONV	1591	1616
POPV-OAV	1592	1614
PONV	1600	1612
PONV-OAV	1605	1607

vibrational energy of the vinyl linkage, a plot of the peak position of the vinyl vibration and EA_{vinyl} of eq 1 is shown in Figure 6. It can be seen that as the substitution of the increasingly conjugated units into the backbone is affected, there is a continuous reduction in the energy of vibration and hence the strength of the bond.

Figure 6 illustrates that the EA_{vinyl} used to approximate the relative conjugation across the vinyl bond is well-correlated with the Raman spectral evidence. It can be seen that as EA_{vinyl} is decreased, there is a notable increase in the vinylene stretch position reinforcing the interpretation that the vinyl bond is being weakened. This plot significantly shows that EA_{vinyl} indeed can be used as an accurate measure of the variation of the vinyl bond as the larger, higher electron affinity units are substituted into the chain. A polymer, being a chain-like structure, will be limited by the weakest link, and thus, the limiting of the conjugation across the vinylene bond will hinder the electron−phonon coupling being distributed across the entire polymer backbone. It is becoming apparent that there is a correlation between the electronic structure and the vibrational activity in the polymer systems, suggesting that the vibrational characteristics can be tailored akin to the electronic structure. It has been demonstrated previously[19] that the Stokes shift, a manifestation of electronic−vibrational coupling, can be correlated to the EA_{total} parameter. By extension, it can be seen from Figure 7 that the Stokes shift is well-correlated with the vinyl bond vibrational energy and that this relationship has origins in the vibrational coupling along the polymer backbone. This ability to tailor the vibrational characteristics of the systems would potentially allow the optimization of the radiative yield through the elimination of the avenues that are open for nonradiative decay. This assumption will be further extended by a quantitative analysis of polymer solutions.

First, the number of observable modes contributing to the electronic−vibrational coupling process is compared to the total number of modes. Figure 8 shows the variation of the maximum number of normal modes available to the carbon skeleton, $3N - 6$,[25] with increasing the molecular weight of the monomer

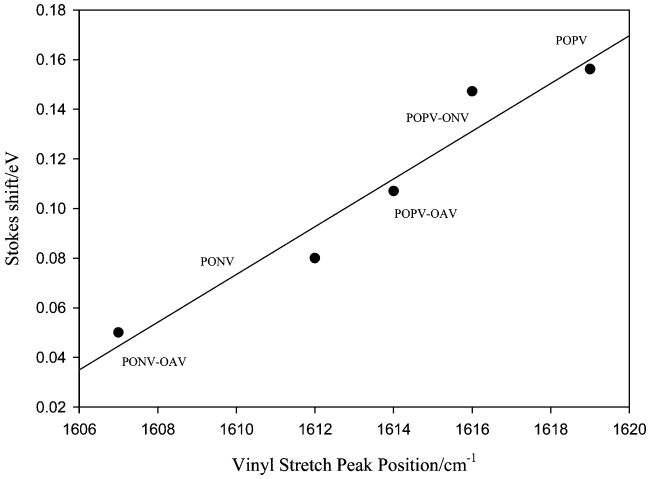

Figure 7. Position of the vinyl stretch plotted against the Stokes shift.

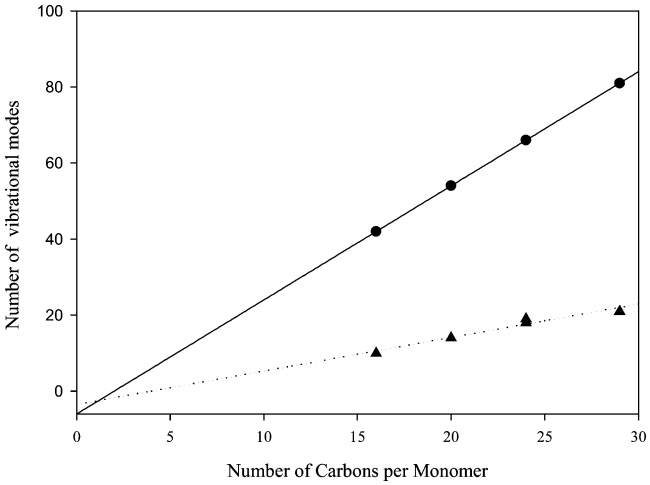

Figure 8. Variation of the number of calculated normal (solid) and experimental Raman (dotted) modes for the carbon backbone.

and also the variation of the number of experimentally observed Raman modes. In the calculation, C−H and side chains are omitted. A monomer is taken to consist of two vinyl bonds and two ring systems in each case. Experimental modes are counted as significant if they are 4% of the maximum observable peak. Since both PONV and POPV-OAV contain the same number of carbons per monomer (24), the points are almost indistinguishable in both experimental and calculated values.

As expected, the number of experimentally observable modes shows a continual increase as the larger more carbon-rich acene units are substituted into the backbone. The rate of increase is low, however, and there is only a small difference between the number of Raman modes present in the POPV and the number of Raman modes present in the PONV-OAV, although the latter contains many more carbon atoms. The maximum variation in the Raman spectra in the series is 13 modes of vibration. In the larger PONV and PONV-OAV, the masked vinyl stretch for both PONV and PONV-OAV is included.

It is notable that the number of observable Raman modes shows a well-defined trend with increasing carbon number. The triangular points in the graph show the plot of the experimental observed peaks exhibiting a slope of ∼1 and an intercept of −3. This can be compared with the plot of the $3N - 6$ calculated modes. As such, it is justifiable to speculate that the Raman spectrum is dominated by the co-operative modes along the length of the carbon backbone. This would give an experimental value of $1N - 3$ for the number of significant modes. This is

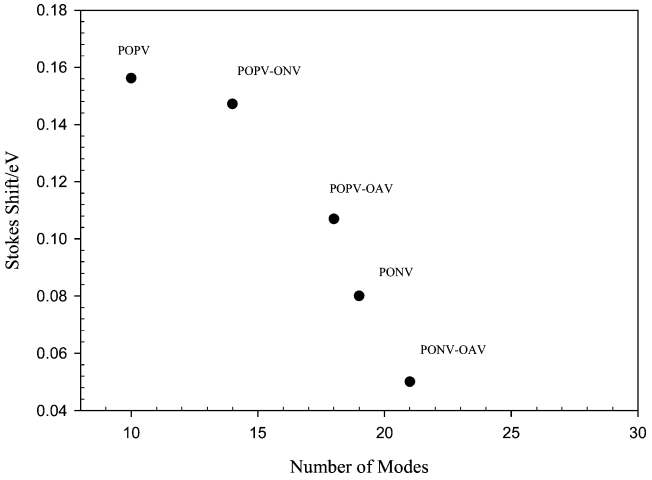

Figure 9. Variation of the Stokes shift with number of observable Raman modes.

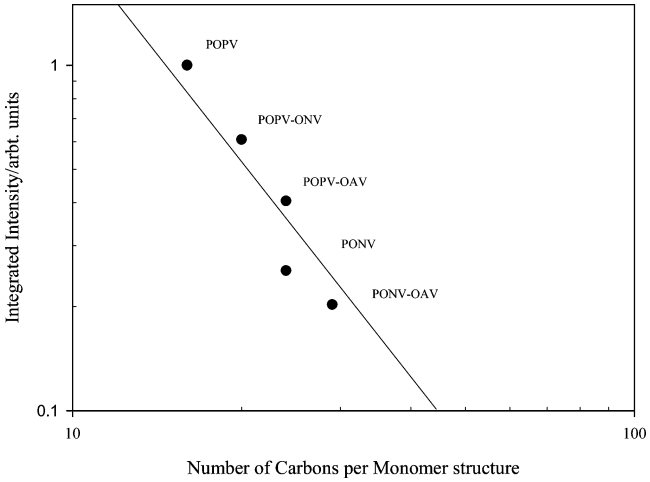

Figure 10. Variation of the integrated Raman intensity with the number of carbons present in the monomer skeleton; solid line shows a slope of −2.

in good agreement with the number of modes that would be calculated for a 1-D linear molecule in which degrees of freedom in the other two dimensions are constrained. Since the intensity of the Raman modes increases with the conjugation length to the fourth power in conjugated oligomers,[15] the observed dominance of these longitudinal modes is not unexpected.

As can be seen from Figure 9, as the number of observable Raman modes is increased, a significant reduction in the Stokes shift is observed. A continuous decrease of the Stokes shift is observed as the larger acene units are substituted into the backbone. It has been shown that acene oligomers show a −6 power law dependence[16] that is not observable here, although the general trend is maintained. The absence of a power dependence can be attributed to the fact that in the polymers, the effective conjugation length is similar for all, and although there is an increase in the number of carbons present per monomer unit through the polymer series, this is negligible in comparison to the number of carbons present in an effective conjugation length. Thus, the number of modes calculated per monomer unit is not an accurate reflection of the number of modes available for the dispersion of the excess excitation energy.

The next step was to quantitatively examine the change in the integrated vibrational intensities as the structural modification was systematically implemented. Figure 10 shows the integrated Raman intensity, from 800−1700 cm^{-1}, plotted against the number of carbons present in the polymer monomer conjugated backbone. The oligomer[15] study was conducted with the integrated Raman intensity going from 100−3200 cm^{-1}, but since the polymers were examined in solution, the integration window had to be limited due to a large chloroform peak at 3100 cm^{-1} and below 800 cm^{-1}. However, this is not a significant problem as it has been shown that the carbon vibrations centered at ∼1600 cm^{-1} provide most of the nonradiative avenues.[26]

It is clearly evident that as the number of carbons is increased, there is a continual decrease in the integrated Raman activity. This is counterintuitive as one would assume that the inclusion of a greater number of carbon−carbon bonds would ultimately lead to an increase of the integrated Raman intensity. The model oligomer systems showed a power of 2 increase with the number of conjugated bonds. If one assumes that the effective conjugation length from all the polymers is approximately the same, it would be expected that the Raman intensity of the polymers containing the anthryl and naphthyl units would have the highest integrated intensity as the acene series showed a power of 2 increase when going from naphthalene to anthracene. The mere inclusion of this should increase the Raman intensity if the polymer was just the sum of its parts. The fact that this is not observed suggests that, as shown for the electronic properties, there is a double effect to be taken into account here. The disruption along the vinyl bond that has been shown[16] must prevent the full active cooperation of the constituent units of the polymers, hence eliminating the super linear behavior demonstrated by the oligomers. The higher electron affinity of the moiety inserted into the chain seems to dictate the degree to which the units contribute across the vinyl bond and hence limit the electron phonon coupling.

To analyze this further, one must examine thoroughly both the electronic disruption created by the insertion of the acene units and the vibrational decoupling of the systems as a result of differing vibrational frequencies of the chain constituents, prohibiting vibrational cooperation. In POPV, there exist both a very strong vinyl linkage and also a frequency matching of the phenyl units, both being at 1581 cm^{-1}. Similar to coupled pendula, this leads to strong vibrational coupling across the polymer backbone and hence a large integrated Raman signal. The next vibrationally well-matched polymer is PONV, which, similar to POPV, has the same conjugated moiety on either side of the vinyl bond. It would be expected that the vibrations would be well-coupled, leading to a strong Raman intensity, increased over that of POPV due to the increased conjugation of the naphthyl unit. However, PONV shows a significant reduction in the integrated Raman intensity that can solely be attributed to the reduced electronic decoupling across the vinylene bond. The spectral evidence that illustrated the softening of the vinylene bond and the electronic analysis shows that this is in fact the case.

The polymers that contain alternating moieties in their backbone makeup show a decrease in Raman activity as well, which can be attributed in part to the electronic disruption across the vinylene bond. However, if this is solely electronic in origin, the reduction in vibrational intensity should have a well-defined relationship with EA_{total}, as this parameter was shown to approximate the electronic variations in the system. In an effort to distinguish between the variation in the Raman intensity due to electronic and vibrational decoupling effects, the integrated Raman intensity is plotted against EA_{total}. A well-defined trend would further advance the postulation that the electronic decoupling of the systems is the dominant effect. It must be

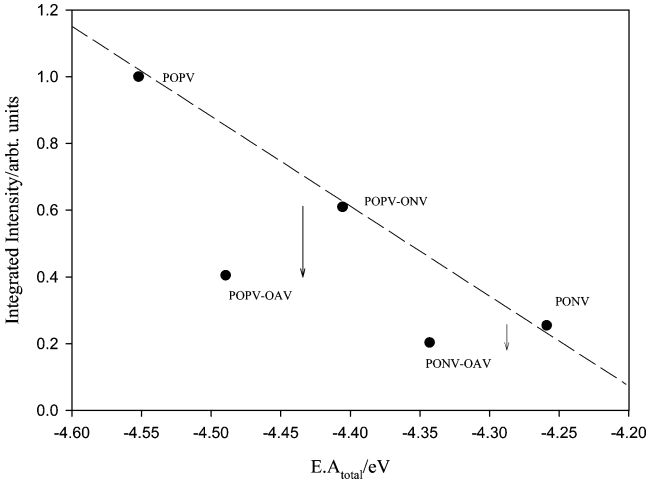

Figure 11. Variation of the integrated intensity against EA_{total}; dotted line is a guide for the eye.

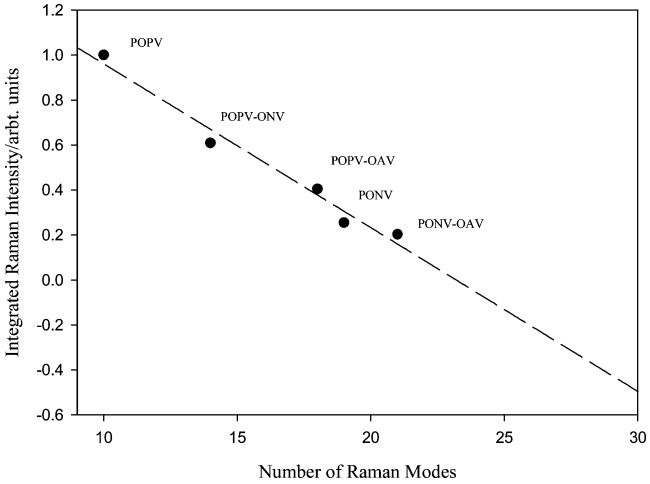

Figure 12. Variation integrated Raman intensity with the number of modes.

noted that EA_{total} takes into account both the variation of the vinyl bond and the increase in the conjugation/vibrational activity of the individual endgroups. It does not, however, account for any effect that would introduce the vibrational decoupling. A variation from a linear trend would indicate vibrational as opposed to electronic decoupling.

In Figure 11, the relative Raman intensity is plotted against the electronic parameter EA_{total}. A dotted straight line is shown, as a guide for the eye, linking the vibrational matched polymers POPV and PONV. The relationships between these polymers have been discussed, and it was concluded that the reason for the reduction of the integrated intensity lies solely with the electronic decoupling across the vinylene bond. Only one other polymer in the series sits on this line, and it is POPV-ONV, which indicates that although there is a vibrational mismatch, the naphthyl stretch being at $\sim$1390 cm^{-1} and the phenyl ring stretch at 1591 cm^{-1}, the electronic change resulting in the vinyl disruption is the dominant factor in the vibrational changes. However, the apparent vibrational mismatch may be softened by the coupling of the naphthyl ring stretch to the ring vibration present at $\sim$1310 cm^{-1}.

The further addition of another fused ring leads to the POPV-OAV polymer, which clearly can be seen to be significantly reduced from the POPV-ONV level of vibrational activity. This deviation can be seen as an indication of the vibrational decoupling between the alternating moieties in the backbone. This behavior is again shown with the addition of another fused ring to PONV, resulting in PONV-OAV. The vibrational mismatch between naphthyl 1395 cm^{-1} and anthryl 1460 cm^{-1} can be seen to provide a reduction in the integrated intensity that cannot be accounted from the purely electronic disruption of the vinyl bond. The disruption of the conjugation resulting in the largest blue-shift of the electronic spectra is evident in PONV. PONV-OAV would fit to the electronic parameters if, as suggested by the increase in integrated intensity with chain length shown by the acene oligomers, the introduction of the higher order acene units provided an increase in intensity regardless of the cooperative effect across the vinyl stretch.

It can be seen that if the disruption of the vinyl linkage was the only factor in the reduction of the vibrational intensity of the polymers with increasing carbon number, then the series should fit well to an electronic parameter (i.e., EA_{total}). However, this parameter fails to take into consideration any effects due to the vibrational mismatching of the alternating units. In the overall effect on the system, it can be seen that the electronic disruption is the major factor, but it also has been illustrated that by decoupling the vibrations through the mismatching of the frequency of vibration, the integrated intensity can be further reduced. Thus, the vibrational characteristics of the polymeric systems can be tailored by disrupting the vibrational coherence of the system.

To further investigate the point that the super linear increase in Raman intensity displayed by the oligomers is curtailed by the weakening of the vinyl bond, the number of experimental Raman modes is plotted against the integrated Raman intensity in Figure 12. It can be seen that although the number of Raman modes is increasing, the integrated intensity is decreasing. This indicates that although the number of modes available is increasing, the lack of vibrational coherence across the vinyl bond restricts the buildup of vibrational intensity.

Evidence that the electron vibrational coupling can be tailored to much the same degree as the electronic characteristics has been demonstrated throughout this paper. The fact that the inclusion of more highly conjugated subsections into the backbone has the effect of lowering the integrated Raman intensity is considerably important in the establishment of structure−property relationships for the vibrational characteristics of complex conjugated systems. Since it has already be shown that the integrated Raman intensity deceases with increasing the number of carbons, it leads on from this that the Raman intensity also decreases as the number of Raman modes is increased.

The main aim of this study was to establish relationships that would allow the systematic control of the electronic and vibrational characteristics of complex polymeric systems. The study to date has shown beyond a reasonable doubt that the vibrational characteristics, shown through Raman spectroscopy, indeed can be modified in a similar fashion to the electronic characteristics. Well-defined trends have been established that correlate well with the already demonstrated relationships outlined for the oligomers.

Ultimately, the end goal was to control the vibrational properties of the polymeric systems in well-structured steps and in doing so work to reduce the electronic−vibrational coupling and thus limit the nonradiative decay, optimizing the fluorescence yield. Figure 13 shows the variation of the normalized fluorescence yield with the integrated Raman intensity. The fluorescence was normalized to the most fluorescent polymer in the series.

It can be seen in Figure 13 that as the integrated Raman intensity is decreased, reducing the vibrational coupling, the yield is continually increased. This is in contrast to the behavior shown by the shorter chain oligomers where there was no definable trend between the vibrational intensity and the

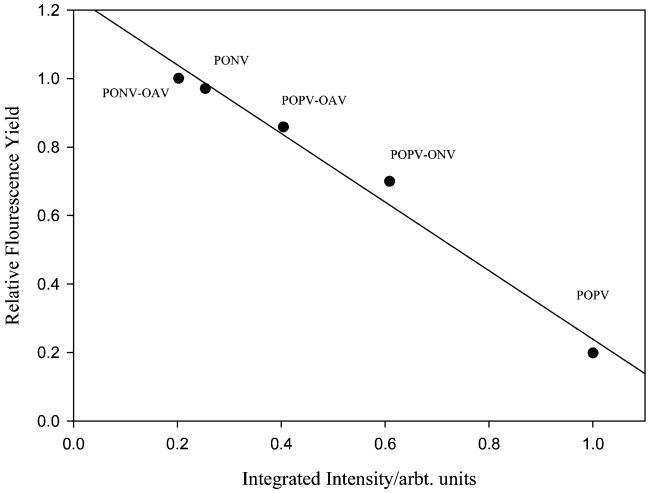

Figure 13. Variation of the fluorescence yield with integrated Raman intensity; solid line is a linear fit.

fluorescence yield.[27,28] This was attributed to the dominant effect of intersystem crossing on the fluorescent yield, and it can be seen that this is not the case in the polymer, which leads to the conclusion that the nonradiative decay becomes the dominant effect in the longer chain polymers. It can be seen that the integrated intensity and yield are inversely proportional, which is further evidence that by disrupting the vinyl bond conjugation, the percentage of available modes, Raman intensity, and Stokes shift are all reduced. Hence, it shows that the Stokes shift can be used as a crude guide to the electronic−vibrational coupling in a polymeric chain, and thus by reducing the Stokes shift, the fluorescence yield is increased. It must, however, be noted that this luminescence increase may be negated in solid state OLED due to the increased prominence of self-absorption as the Stokes shift is reduced. It is, however, evident that the Raman activity is a far superior tool to gauge the electron vibrational coupling along the backbone and that reducing this will ultimately lead to a greater yield, provided the nature of the conjugation is maintained.

Conclusion

The aim of this paper was to explore the vibrational characteristics of a series of novel π-conjugated polymers. It has been previously shown that systematically changing the order of the acene moiety substituted into the backbone leads to clearly defined structure−property relationships for the electronic properties. These relationships were found to be similar to those well-established for electronic processes in short chain oligomers. Having established well-defined structure−property relationships for the absorption and emission, the next step was to explore the possibility of a well-defined vibrational relationship that could be elucidated by such a systematic analysis.

It has been shown throughout that well-defined vibrational characteristics exist for π-conjugated polymers. The ultimate goal of this study was to explore the vibrational relaxation of the complex polymeric systems in an attempt to control radiative decay and hence optimize the fluorescence yield. This has been shown for the series of polymers examined. However, in the study, it was evident that the separation of the electronic and vibrational effects in such a system was not a trivial matter. The goal was to minimize the vibrational activity of the system by controlling the vibrational activity of the system through a process of decoupling the vibrational frequencies. What is evident is that the introduction of the larger acene units into the backbone had the effect of reducing the vibrational coherence along the backbone but also a larger electronic effect. The two effects can be summed as the weakening of the vinyl bond through the introduction of groups less likely to participate fully across the vinylene and the desired effects of reducing the electron coupling through decoupling the oscillators along the polymer chain. It was shown that both effects are present but that the dominant effect is electronic in nature and results from the changing electronic affinity of the acene groups incorporated into the backbone.

Regardless of the nature of decoupling of the electronic and vibrational states, the end result is highly significant. Through limitation of the vibrational activity of the systems, it is possible to limit the nonradiative decay and hence optimize the fluorescence yield of the systems in question.

Acknowledgment. The FOCAS Institute is funded under the National Development Plan 2000−2006 with assistance from the European Regional Development Fund. L.O. acknowledges DIT Scholarship support.

References and Notes

(1) Yu, G.; Wang, J.; McElavin, J.; Heeger; A. J. *Adv. Mater*. **1998**, *10* (17), 1431.

(2) Sariciftci, N. S. *Curr. Opin. Solid State Mater. Sci.* **1999**, *4* (4), 373.

(3) Chen, L.; McBranch, D. W.; Wang, H. W.; Helgeson, R.; Wudl, F.; Whitten, D. G. *Proc. Natl. Acad. Sci. U.S.A.* **1999**, *96* (22), 12287.

(4) Sirringhaus, H.; Tessler, N.; Friend, R. H. *Science* **1998**, *280*, 1741.

(5) Schwartz, B. J.; Hide, F.; DiazGarcia, M. A.; Andersson, M. R.; Heeger, A. J. *Philos. Trans. R. Soc. London, Ser. A* **1997**, *355*, 775.

(6) Sauteret, C.; Hermann, J. P.; Frey, R.; Pradere, F.; Ducuing, J.; Baughman, R. H.; Chance, R. R. *Phys. Rev. Lett.* **1996**, *36*, 956.

(7) Rustagi, K. C.; Ducuing, J. *Opt. Commun.* **1974**, *10* (3), 258.

(8) Burroughes, J. H.; Bradley, D. D. C.; Brown, A. R.; Marks, R. N.; Mackay, K. D.; Friend, R. H.; Burns, P. L.; Holmes, A. P. *Nature* **1990**, *347*, 539.

(9) Friend, R. H.; Gymer, R. W.; Holmes, A. B.; Burroughes, J. H.; Marks, R. N.; Taliani, C.; Bradley, D. D. C.; Dos Santos, D. A.; Logdlund, M.; Salaneck, W. R. *Nature* **1999**, *397* (6715), 121.

(10) Wegmann, G.; Giessen, H.; Greiner, A.; Mahrt, R. F. *Phys. Rev. B* **1998**, *57*, 4218.

(11) Drexhage, K. H. *J. Res. Natl. Bureau Standards, Sect. A* **1976**, *80* (3), 421.

(12) Stalmach, U.; Detert, H.; Meier, H.; Gebhardt, V.; Haarer, D.; Bacher, A.; Schmidt, H.-W. *Opt. Mater.* **1998**, *9* (1−4), 77.

(13) Tian, B.; Zerbi, G.; Schenk, R.; Mullen, K. *J. Chem Phys.* **1991**, *95* (5), 3191.

(14) Shaui, Z.; Bredas, J. L.; Su, W. P. *Chem. Phys. Lett.* **1994**, *228* (4−5), 301.

(15) O'Neill, L.; Byrne, H. J. *J. Phys. Chem. B* **2005**, *109*, 12685.

(16) O'Neill, L.; Lynch, P.; McNamara, M.; Byrne, H. J. *J. Phys. Chem. A* **2007**, *111* (2), 299.

(17) Meier, H. *Angew. Chem., Int. Ed.* **2005**, *44*, 2482.

(18) Meier, H.; Muhling, B.; Kolshorn, H. *Eur. J. Org. Chem.* **2004**, *27*, 1033.

(19) Lynch, P.; O'Neill, L.; McNamara, M.; Byrne, H. J. *Macromolecules*, submitted.

(20) Maier, S. Ph.D. Thesis, University of Dublin Trinity College, Dublin, Ireland, 2000.

(21) O'Neill, L. Ph.D. Thesis, Dublin Institute of Technology, Dublin, Ireland, 2007.

(22) Socrates, G. *Infrared and Raman Characteristic Group Frequencies: Tables and Charts*, 3rd ed.; Wiley: New York, 2004.

(23) Zeng, Q. G.; Ding, Z. J.; Tang, X. D.; Zhang, Z. M. *J. Lumin.* **2005**, *115*, 32.

(24) Zheng, G.; Clark, S. J.; Tulip, P. R.; Brand, S.; Abram, R. A. *J. Chem. Phys.* **2005**, *123*, 24904.

(25) Vincent, A. *Molecular Symmetry and Group Theory*; Wiley: New York, 1977.

(26) Karabunarliev, S.; Bittner, E. R.; Baumgarten, M. *J. Chem. Phys.* **2001**, *114*, 5863.

(27) Birks, J. B. *Photophysics of Aromatic Molecules*; Wiley: New York, 1977.

(28) Pope, M.; Swanberg, C. *Electronic Processes in Organic Crystals and Polymers*; Oxford University Press: Oxford, 1999.